Macromolecules **1992,** *25,* 6885–6890

Solution Properties of Polar Modified Poly(styrene-*co*-isoprene)

Jochen Stock[†] **and Walther Burchard**

Institut für Makromolekulare Chemie, Albert Ludwigs Universität Freiburg,
Stefan Meier Strasse 31, D-7800 Freiburg, Germany

Reimund Stadler*

Institut für Organische Chemie, Johannes Gutenberg Universität Mainz,
J. J. BecherWeg 18-20, D-6500 Mainz, Germany

Received December 18, 1991; Revised Manuscript Received August 26, 1992

ABSTRACT: A statistical copolymer of styrene and isoprene was modified with polar phenylurazole groups which are able to form binary hydrogen complexes. The solution properties of the unpolar polymer backbone with polar side groups were examined. Effects of the degree of modification were studied in dilute and semidilute solution by light scattering (static and dynamic), viscosity, and IR spectroscopy. Association of the system was found to occur in several steps from very small aggregates to gellike systems. The dissolved aggregates show a behavior which is typical for compact or spherelike particles in solution. From the combination of IR spectroscopy and light scattering it can be concluded that most of the binary complexes lead to intramolecular ring formation and are not available for intermolecular association. This may explain the observed compact structures.

Introduction

Stable junctions in a reversible gelling system are often formed by cooperative incorporation of many repeating units into spatially extended junction zones. Different types of intermolecular forces like hydrogen-bond, dipole, ionic, or hydrophobic interactions induce the formation of junction zones, stabilize them, and may eventually cause gelation.[1–6]

Many different chemical concepts have been described which show reversible network formation in synthetic systems. Ionomers are typical examples of this class of gel-forming polymers.[7,8] The complex nature of ionic clusters prevents largely the detailed understanding of reversible gels. The access to theoretical models is restricted because the structure and size of the ionic clusters in bulk as well as in solution are still a matter of intense scientific debate. Most theoretical work is based on the assumption of *pointlike* interactions between *two* groups, which is not true for ionomers or biological gels.

In the past we have developed a synthetic model[9–13] where the following conditions were realized: (a) defined type of interaction (formation of binary hydrogen-bond complexes); (b) controlled variation of the number of interacting groups per chain; (c) use of polymers of narrow molecular weight distribution; (d) independent characterization of the hydrogen-bond interactions on a microscopic level. These conditions were realized by the introduction of "urazole" groups into a polydiene via an ene reaction. The number of urazole groups per chain can be varied either by changing the primary molecular weight or the degree of substitution. Two urazole groups form a defined chelatelike hydrogen-bond complex (Figure 1). From IR spectroscopy information of the effective number of junctions is available.

A detailed rheological characterization was performed with urazole-modified polybutadienes.[14–16] In accordance with theoretical considerations, deviations from the behavior of a "true" or "ideal" network were observed.

The present study focuses on the aggregation of such a model system in a dilute and semidilute solution.

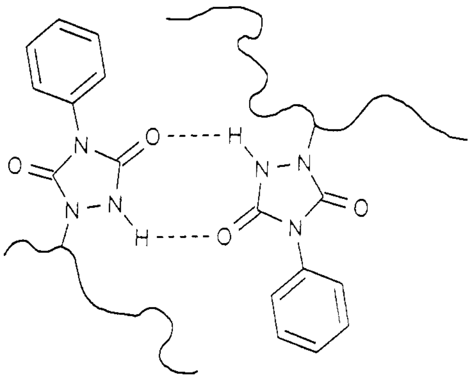

Figure 1. Binary hydrogen-bond complex formed by two interacting phenylurazole groups.

Experimental Section

1. **Materials and Sample Preparation.** Because of the large amount of data available in the literature[17] on the solution behavior of polystyrene (while the data basis for the solution properties of polydienes is much narrower), we chose a polystyrene-based system.

A statistical copolymer of styrene and isoprene P(S-*co*-I) was prepared by anionic polymerization in cyclohexane (with 5 vol % triethylamine) with *n*-butyllithium as initiator. The weight fraction of isoprene was 11.8%. The molecular weight and nonuniformity $U = M_w/M_n - 1$ were determined by different methods. The results, which are collected in Table I, are in good agreement within experimental error. Due to the presence of the amine, the copolymerization behavior of the monomer pair is close to an ideal azeotropic copolymerization.

4-Phenyl-1,2,4-triazoline-3,5-dione (PTD) was synthesized according to literature prescriptions.[18–21] The introduction of the functional urazole groups by addition of the triazolinediones is described elsewhere.[22–24] The samples used throughout this study are listed in Table II.

2. **Light Scattering Experiments.** The light scattering measurements were carried out using an apparatus that allows the simultaneous recording of static and dynamic light scattering. The experiments were performed in toluene as a solvent at 20 °C using a wavelength $\lambda_0 = 496.5$ nm and an angular range from 20° to 150° in steps of 10°. Experiments were performed in a concentration range from 0.3 to 240 g/L, varying for different samples.

3. **Refractive Index Increment.** The refractive index increments d*n*/d*c* were determined using a Brice-Phoenix dif-

---

[†] Present address: Institut für Organische Chemie, Johannes Gutenberg Universität Mainz, J. J. BecherWeg 18-20, D-6500 Mainz, Germany.

0024-9297/92/2225-6885$03.00/0

Table I
Characterization of the Original Copolymer P(S-*co*-I)

method	M_w	M_n	U
light scattering	5.38×10^4		0.02
membrane osmometry		5.30×10^4	
GPC (IR detection)	5.78×10^4	5.42×10^4	0.07
GPC (UV detection)	5.95×10^4	5.30×10^4	0.12

Table II
Designation of Functionalized Samples[a]

sample	isoprene (mod.)	N_u/N_m	N_u
P(S-*co*-I)			0
P(S-*co*-I)–PU-20	20	0.034	18
P(S-*co*-I)–PU-45	45	0.077	41
P(S-*co*-I)–PU-60	60	0.102	55
P(S-*co*-I)–PU-90	90	0.153	82

[a] Isoprene (mod.): Percentage of functionalized isoprene units (mol %). N_u/N_m: Mole fraction of repeating units carrying functional groups. N_u: Number of urazole units per chain (calculated from the molecular weight of the unmodified copolymer and the added amount of PTD).

Table III
Characterization of Dilute-Solution Behavior

sample	M_w	A_2 (mol·cm^3/g^2)	R_g (nm)	D_z (cm^2/s)	$[\eta]$ (g/cm^3)
P(S-*co*-I)	5.38×10^4	7.64×10^{-4}	12.3	6.09×10^{-7}	34.3
P(S-*co*-I)–PU-20	6.64×10^4	5.91×10^{-4}	11.9	6.01×10^{-7}	27.7
P(S-*co*-I)–PU-45	7.47×10^4	4.35×10^{-4}	14.4	6.38×10^{-7}	25.2
P(S-*co*-I)–PU-60	8.69×10^5	1.37×10^{-4}	29.5	4.00×10^{-7}	22.4
P(S-*co*-I)–PU-90	3.40×10^6	4.69×10^{-5}	36.7	1.53×10^{-7}	20.2

Table IV
Experimental and Theoretical Values of the Molecular Weight Dependence of Radius of Gyration a_{R_g}, Diffusion Coefficient a_D, Viscosity a_η, and Second Virial Coefficient a_{A_2}

exponent	good solvent (coil)	θ solvent (coil)	hard sphere	polystyrene[31]	P(S-*co*-I)–PU-*x*
a_{R_g}	0.6	0.5	0.33	0.595	0.321
a_D	−0.6	−0.5	−0.33	−0.578	−0.293
a_η	0.8	0.5	0	0.788	−0.098
a_{A_2}	−0.2			−0.203	−0.639

ferential refractometer at five different wavelengths (647.1, 611.0, 580.0, 546.0, and 496.5 nm). The experimental data of d*n*/d*c* for each wavelength λ were plotted versus λ^2. The final value of d*n*/d*c* at λ = 496.5 nm was determined from linear regression of this relation. For all samples a value of 0.100 mL/g (±3%) was found.

Solutions for light scattering and d*n*/d*c* measurements were prepared at least 1 day before use to allow time for equilibration. All solutions were filtered through 0.45-μm Millipore filters three times before filling into dust-free LS cells. Laboratory-grade toluene was dried over sodium wire before use.

4. FTIR Spectroscopy. IR spectra were obtained using a Bruker IFS48 equipped with a Specac variable-temperature cell; the spectra were taken at a resolution of 2 cm^{-1}; 32 scans were accumulated. To study the changes in the range of the carbonyl absorption of the urazole ring, a solution of the unmodified polymer in toluene was used to obtain the single-channel reference spectrum. The absorption spectra of the modified polymers were obtained from the corresponding single-channel spectra and this reference spectrum.

5. Viscosity Measurements. The viscosity measurements were carried out using an automatically operating Schott AVS/G viscosimeter system. The solutions were filtered through Millipore filters (0.45 μm).

Results and Discussion

Dilute-Solution Behavior (Table III). The static light scattering data were evaluated according to Zimm,[25,26] while the hydrodynamic radii were analyzed by the method of cumulants.[27-29] The experimentally available time correlation function TCF is expressed in the following manner:

$$g_1(t) = \exp(-D_q{}^2 t) \qquad (1)$$

where $g_1(t)$ denotes the TCF, t the decay time, q the scattering vector, and D the diffusion coefficient. The decay constant may be expressed by eq 2. In many cases

$$\Gamma = Dq^2 \qquad (2)$$

it is useful to describe TCF in terms of a cumulant expansion:[28-29]

$$\ln g_1(t) = \Gamma_1 t + (\Gamma_2/2!)t^2 - (\Gamma_3/3!)t^3 + \ldots = \Gamma t \qquad (3)$$

In this study the TCF was adequately described by a two-cumulant fit. The value of Γ/q^2, which in general is concentration and angular dependent, only shows a concentration dependence in the present system. The diffusion coefficient D_c was obtained as the mean value over all angles. The translational diffusion coefficient D_z can be determined by extrapolation to zero concentration (eq 4).[29]

$$D_c = D_z(1 + k_D c) \qquad (4)$$

Values of M_w were obtained by extrapolation to zero concentration and A_2 calculated from the initial slope of $Kc/R_{\theta=0}$ as a function of concentration (see eq 6). The sample P(S-*co*-I)–PU-60 shows a sharp decrease in the scattering intensity for very low concentrations. Therefore, A_2 and M_w could only be estimated from three data points within the region from 3 to 5 g/L. D_c on the other hand increases very rapidly for low concentrations so that extrapolation to zero concentration according to eq 4 may be erroneous for P(S-*co*-I)–PU-60. For this reason the value of D_z was also taken from extrapolation at higher concentrations. Determination of R_g is not satisfactory for the samples P(S-*co*-I), P(S-*co*-I)–PU-20, and P(S-*co*-I)–PU-45 because the observed values of the radii of gyration are close to the experimental limit where the angular dependence of the scattering intensity is detectable.

Viscosity data as a function of concentration are extrapolated to infinite dilution by means of the Huggins equation:[30]

$$\eta_{sp}/c = [\eta] + k_H[\eta]^2 c \qquad (5)$$

The modified polymers show significant deviations from the behavior of linear flexible chains in a good solvent. These deviations are increasing with an increasing number of polar groups per chain.

Validity of the scaling relations for dilute solutions of linear chains is restricted to molecularly dissolved, flexible polymer chains.[32] This condition is no longer fulfilled for the modified copolymer. Therefore, it is not surprising that deviations are strong for high degrees of substitution. The fact that the experimental exponents a_{R_g} and a_η are lower than for linear chains, while a_{D_z} takes higher values, indicates that the substituted P(S-*co*-I)–PU-*x* polymers behave similar to collapsed coils. If the experimental quantities are compared with theoretical predictions for hard spheres, the values are in reasonable agreement (see Table IV), while the molecular weight dependence of A_2 (according to an exponent $a_{A_2} = -0.64$) shows a quantity which has been reported in the literature for associating polymer systems ($a_{A_2} = -[0.5–0.7]$).[33,34] However, this discussion of the dilute-solution behavior has been based

Table V
Theoretical Molecular Weights of the Individual Chain (M_{w0}) and Molecular Weights Obtained from Light Scattering (M_w) in the Dilute Regime (for Details of Extrapolation, See Text)

sample	M_{w0}	M_w	M_w/M_{w0}
P(S-*co*-I)	5.38×10^4	5.38×10^4	1
P(S-*co*-I)–PU-20	6.26×10^4	6.64×10^4	1.06
P(S-*co*-I)–PU-45	6.71×10^4	7.47×10^4	1.11
P(S-*co*-I)–PU-60	6.97×10^4	86.9×10^4	22.1
P(S-*co*-I)–PU-90	7.16×10^4	340×10^4	47.5

[a] M_{w0}: Calculated molecular weight after chemical modification, based on the measured M_w of P(S-*co*-I) and the added amount of functional groups.

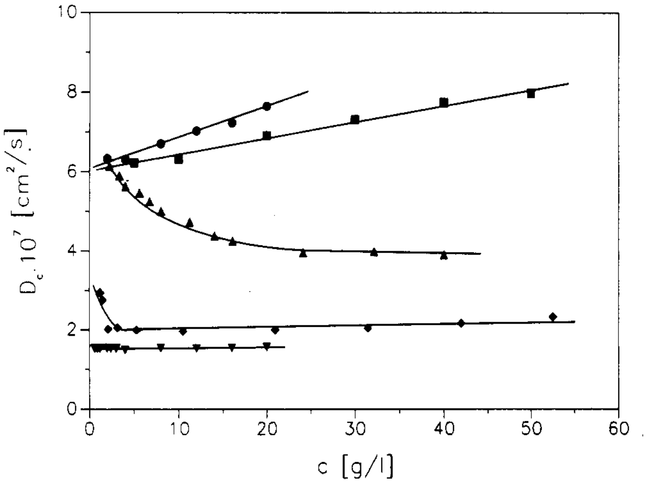

Figure 2. Apparent diffusion coefficient D_c as a function of concentration: (●) P(S-*co*-I), (■) P(S-*co*-I)–PU-20, (▲) P(S-*co*-I)–PU-45, (◆) P(S-*co*-I)–PU-60, (▼) P(S-*co*-I)–PU-90.

on the assumption of a *molecularly* dispersed system, which is not true for all samples. The molecular weight of the "real" single chain can be very easily calculated from the molecular weight of the unmodified polymer plus the added amount of PTD (listed in Table V as M_{w0}).

For the lower degrees of modification, P(S-*co*-I)–PU-20 and P(S-*co*-I)–PU-45, extrapolation of $Kc/R_{\theta=0}$ to zero concentration gives values which are in agreement (within the range of experimental error) with the expected single-chain behavior (see Table V). It must be concluded that dilute-solution (single-chain) behavior is observed for these samples in the low concentration regime. With increasing number of urazole units per chain the ratio of measured to calculated molecular weight M_w/M_{w0} (Table V) increases. Obviously no "dilute solution" in the common sense is present even in the low concentration regime. The properties of the solution are governed by the formation of aggregates. As a first tentative proposal for the solution structure in this regime we suggest the existence of a "dilute solution" of clusters with finite molecular weight (and probably with a broad molecular weight distribution). Further evidence for this suggestion will be obtained from the study of the concentration dependence.

Concentration Dependence of the Diffusion Coefficient. A plot of the diffusion coefficient D_c as a function of concentration is shown in Figure 2.

The original copolymer P(S-*co*-I) and the sample with the lowest degree of substitution show a linear concentration dependence with a slope $k_D D_z > 0$; however, the slope for P(S-*co*-I)–PU-20 is already strongly reduced. The same value of $D_z = 6 \times 10^{-7}$ cm^2/s is obtained for both samples after extrapolation to zero concentration. All the other samples behave differently.

For concentrations larger than 15 g/L sample P(S-*co*-I)–PU-45 reaches an almost constant value of D_c; i.e., k_D in eq 2 becomes zero, but for lower concentrations k_D is negative. Again, from extrapolation to $c = 0$, D_z approaches the value of the single chain. The apparent diffusion coefficients D_c for P(S-*co*-I)–PU-60 are concentration independent down to concentrations of 0.9 g/L. An increase of D_c is observed for lower concentrations, but within the concentration range where reliable light scattering data could be obtained, the value of D_z only rose from 2×10^{-7} to 3×10^{-7} cm^2/s for P(S-*co*-I)–PU-60. Thus it is evident that no single-chain behavior was reached for this sample. For the highest degree of modification the apparent diffusion coefficient is concentraton independent over the whole concentration range. The value of $D_z = 1.5 \times 10^{-7}$ cm^2/s again is considerably lower than the value expected for a single chain.

The concentration dependence of D_c can no longer be described by eq 4 for the highly modified sample. The coefficient k_D becomes a function of concentration $k_D(c)$.

These concentration-dependent diffusion data support the interpretation of the dilute-solution data and give strong evidence for intramacromolecular as well as intermacromolecular association between the polar urazole groups.

Concentration Dependence of Static Light Scattering. In the following the concentration-dependent static forward light scattering will be analyzed. We attempt to get further information about the structure of the semidilute solutions in this association system. In Figure 3 forward scattering $Kc/R_{\theta=0}$ is shown for all samples.

The unsubstituted basic copolymer shows no deviations from Zimm type behavior. Equation 6 remains valid over the whole concentration range. K denotes the optical

$$\frac{Kc}{R_{\theta=0}} = \frac{1}{M_w} + 2A_2c \qquad (6)$$

contrast factor and $R_{\theta=0}$ the forward scattering intensity.

For the polymer with the lowest degree of substitution, P(S-*co*-I)–PU-20, a slight deviation from linear behavior can be detected at higher concentrations. The observation of a nonzero A_3 indicates that even at moderate polymer concentrations polymer–polymer interactions have to be taken into account for a quantitative description of the solution behavior (eq 7). For samples with a larger number

$$\frac{Kc}{R_{\theta=0}} = \frac{1}{M_w} + 2A_2c + 3A_3c^2 \qquad (7)$$

of polar groups per chain the forward scattering intensity shows a complex behavior, which cannot be described by eq 6 or eq 7.

For P(S-*co*-I)–PU-45 $Kc/R_{\theta=0}$ initially increases in the dilute regime. At a concentration of about $c = 5$ g/L the reciprocal scattering intensity suddenly bends down, passing through a minimum. Further increase of the concentration results in a strong nonlinear enhancement of the forward scattering intensity. Sample P(S-*co*-I)–PU-60 shows a similar forward scattering behavior for concentrations above 4 g/L. At lower concentration a strong increase of $Kc/R_{\theta=0}$ is observed.

Sample P(S-*co*-I)–PU-90 does not develop this strong increase in the observed concentration range. The molecular weight extrapolated from the data to $c = 0$ is now about 50 times larger than that for the unmodified copolymer. Nevertheless a maximum and a minimum are detected in the reciprocal scattering.

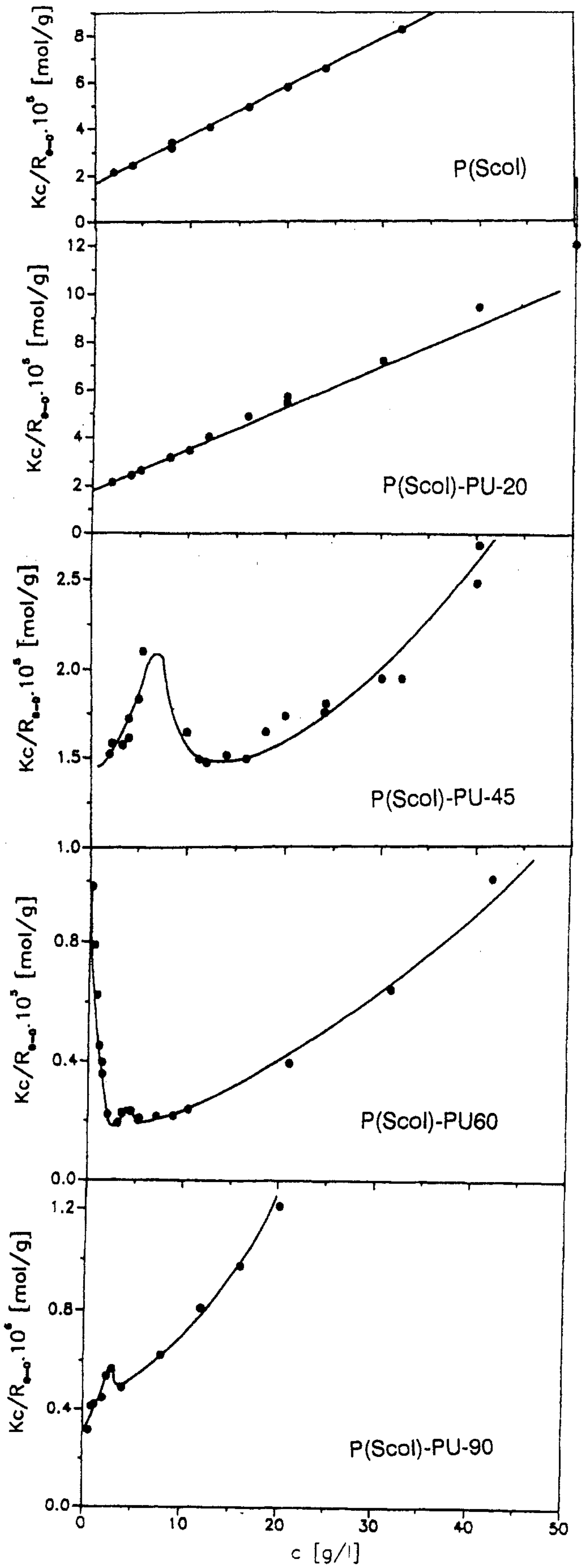

Figure 3. Forward light scattering $Kc/R_{\theta=0}$ as a function of concentration for all samples.

In summarizing these results we have to conclude that different structures form in solution depending on the concentration and degree of modification. Figure 4 gives a hypothetical curve for the forward scattering of such chains with stickers. $Kc/R_{\theta=0}$ is plotted versus cN_u^a to emphasize that the scattering behavior depends on concentration c and the number of urazole groups per chain N_u. The exponent a is an arbitrary constant to put concentration and the functionalization onto the same axes.

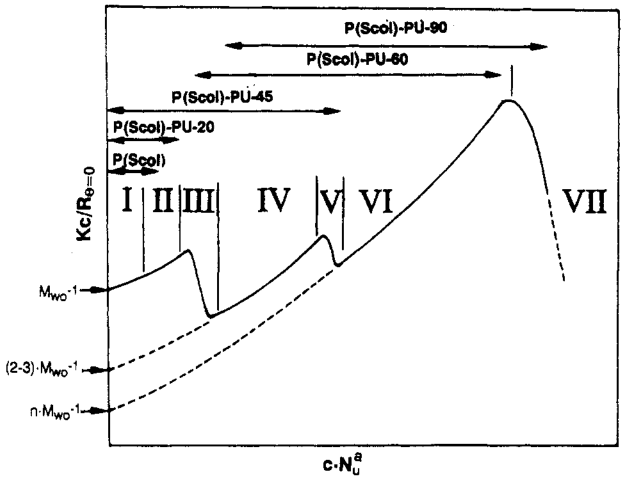

Figure 4. Schematic plot of the forward scattering intensity versus concentration and degree of modification.

Region I corresponds to the typical behavior of an "ideal" dilute solution (eq 6), while region II corresponds to a solution behavior where the third virial coefficient cannot be neglected. In regime III a decrease in the forward scattering intensity indicates the onset of association due to a decrease in the osmotic modulus. Extrapolation of the scattering data of region IV to zero concentration results in an apparent molecular weight which is about 2 times the individual macromolecule. This region correlates to these concentrations, where repulsive forces between primary aggregates are dominating. For higher concentrations these small clusters seem to associate to much larger clusters (region V), which also show a strong repulsion (region VI). In the last regime M_{app} $\{=(Kc/R_{\theta=0})^{-1}\}$ seems to grow to infinity. The samples in the cuvettes become gellike. The bars in Figure 4 correspond to the different regimes realized by the functionalized styrene–isoprene copolymer.

The reduced forward scattering intensity $M_wKc/R_{\theta=0}$ depends on molecular weight, concentration, and molecular architecture.

The quantitative relations $M_wKc/R_{\theta=0} = M_w/M_{app} = f(A_2, M_w, c, \text{architecture})$ have been derived for different topologies.[35] As an example P(S-*co*-I)–PU-45 will be analyzed according to these concepts in more detail. Figure 5 compares the experimental data of P(S-*co*-I)–PU-45 with the theoretical data for flexible coils (broken line) and hard spheres (solid line). At low concentrations the experimental data follow the theoretical predictions. In this regime it is not possible to distinguish between the different architectures. At $A_2M_wc = X = 0.2$ the values of M_{w0}/M_{app} bend down and after passing a minimum start growing again. The curvature resembles the behavior predicted for hard spheres, but the values of M_{w0}/M_{app} are shifted to higher values of X (which means to higher molecular weights). Such a behavior can be explained by a concentration-dependent molecular M_w (and therefore

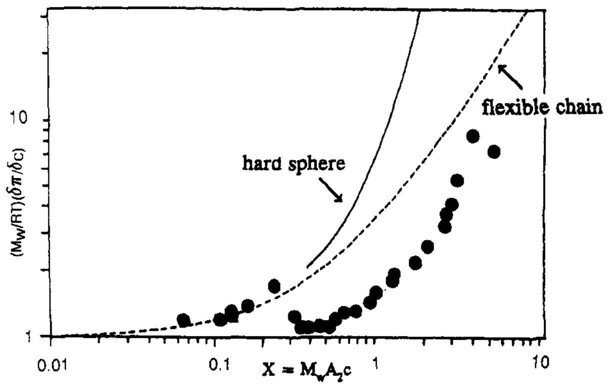

Figure 5. Reduced osmotic modulus as a function of the scaling parameter $X = M_wA_2c$ for the sample P(S-*co*-I)-PU-45: (solid line) theoretical prediction for hard spheres;[43] (dashed line) theoretical prediction for flexible coils.[44]

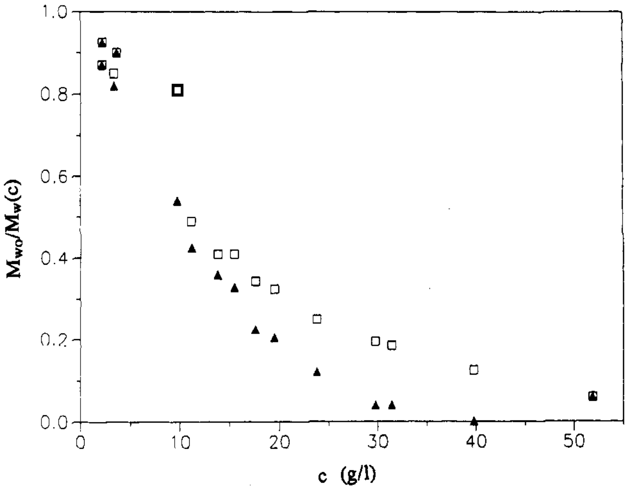

Figure 6. Reduced concentration-dependent molecular weight $M_{w0}/M_w(c)$ as a function of concentration for the sample P(S-*co*-I)-PU-45. The filled triangles show calculations based on model a; the open squares represent the ones for model b. M_{w0} is the molecular weight extrapolated to $c = 0$ ($M_{w0} = 7.47 \times 10^4$).

A_2) for associating species. This circumstance can be taken into account by writing eq 7 to

$$Kc/R_{\theta=0} = \frac{1}{M_w(c)}[1 + 2A_2(c)\,M_w(c)\,c + 3A_3(c)\,M_w(c)\,c^2 + ...] \quad (8)$$

where $A_i(c)$ and $M_w(c)$ denote the "true" virial coefficients and the "true" molecular weight at a certain concentration. For large molecules A_2 is related to M_w by the scaling law $A_2 = K_aM_w{}^a$ and eq 8 takes the form

$$Kc/R_{\theta=0} = \frac{1}{M_w(c)}[1 + 2\{K_aM_w(c)^{1-a}\}c + 3g\{K_aM_w(c)^{1-a}\}^2c^2 + ...] \quad (9)$$

For special models the relationship of eq 9 simplifies considerably, and analytic solutions are possible. Two different models to calculate $M_w(c)$ have been reported: (a) association via closely packed spheres, (b) random association. Details of these calculations are reported in previous publications.[35-43] Figure 6 compares the concentration-dependent molecular weights for these two models for P(S-co-I)-PU-45. For concentrations of about 40-50 g/L both models predict molecular weights approaching infinity, i.e., gelation.

The combination of experimental data and this simple model gives the possibility of estimating the effective or true molecular weight at a certain concentration. With the knowledge of the molecular weight of the clusters at an arbitrary concentration and the molecular weight of a single chain the probability of effective intermolecular bond formation α_{eff} can be determined.[44,45] The total extent of complexation of polar groups α_t can be measured directly by IR spectroscopy (Table VI). Details of the analysis of urazole complex formation are described elsewhere.[46,47] In combination with the Flory-Stockmayer theory,[44,45] it is possible to estimate the fraction of intramolecular rings. Ring formation means that a certain fraction of complexes is formed within an individual chain forming loops. The following two assumptions are fulfilled in the present model system: (a) Every chain contains f functional groups which are capable of forming a junction. (b) Association is a consequence of the formation of binary complexes ($U + U \rightleftharpoons U_2$); U = urazole unit. According to Flory-Stockmayer theory, the concentration-dependent molecular weight is given by

$$M_w(c) = M_{w0}\frac{1 + \alpha_{\text{eff}}}{1 - \alpha_{\text{eff}}(f - 1)} \quad (10)$$

where the following mean-field assumption was made:

$$\alpha_{\text{eff}} = \alpha_t(1 - r), \quad r = \text{fraction of rings} \quad (11)$$

By using the experimental data the experimental fraction

Table VI
Fraction of Urazole Units Involved in Binary Complexes for Several Concentrations According to Quantitative IR Spectroscopy (Polymer, P(S-*co*-I)-PU-60)[a]

concn c_i (g/L)	concn c_{iu} (mol/L)	α_t
52.5	0.047	0.85
31.5	0.028	0.81
21.0	0.019	0.76

[a] c_i: polymer concentration. c_{iu}: concentration of urazole units per volume of solution. α_t: fraction of urazole units involved in complexes.

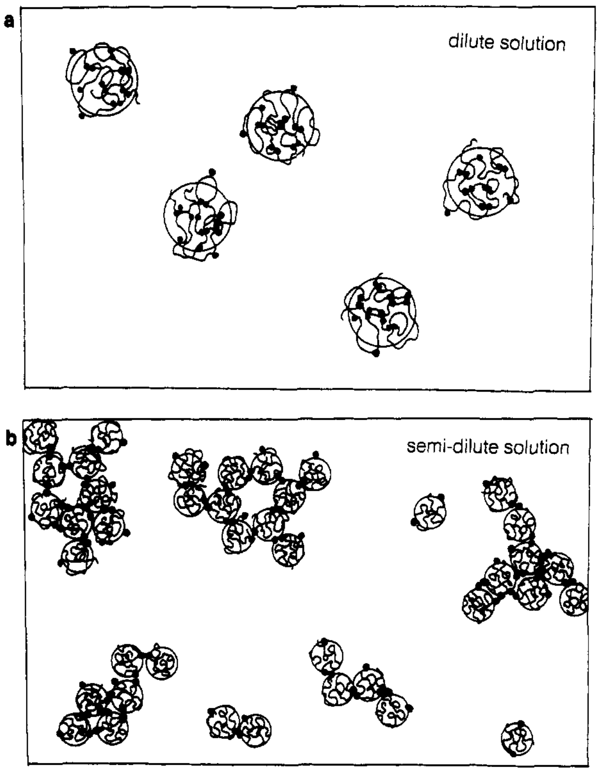

Figure 7. (a) Schematic picture of the spherelike, isolated particles at low concentrations and low degrees of substitution. (b) At higher concentration the preformed collapsed coils aggregating to clusters containing a lot of spherelike particles.

of rings (intramolecular complexes) is on the order of 96–98%. This explains the very compact structure of the aggregates.

These results allow us to give a very schematic picture of the solution properties of polymers containing stickers for binary aggregation (Figure 7).

At very low concentration and with a small number of polar groups per chain the polymer chains are molecularly dissolved. With increasing amount of polar groups the coils become more and more compact due to the formation of intramolecular complexes but they are still molecularly dissolved. At low concentrations this internal clustering will be favored due to the spatial neighborhood of the polar groups. With increasing polymer concentration the probability of contact formation between urazole units on the surface of different collapsed coils increases. As a result dense clusters of large finite molecular weights are formed. Further increase of the concentration results in cluster growth and gelation.

Acknowledgment. This work is supported by the Deutsche Forschungsgemeinschaft through SFB60 (University of Freiburg) and through a Gerhard-Hess grant for R.S. J.S. acknowledges the receipt of a "Kekule-Stipendium" of the Stipendienfonds des Verbands der Chemischen Industrie.

References and Notes

(1) Abe, K.; Tsuchida, E. *Adv. Polym. Sci.* **1982**, *45*, 4.
(2) Clark, A. H.; Ross-Murphy, S. B. *Adv. Polym. Sci.* **1987**, *83*, 57.
(3) Burchard, W.; Stadler, R.; de Lucca Freitas, L.; Möller, M.; Omeis, J.; Mühleisen, E. In *Biological and Synthetical Networks*; Kramer, O., Ed.; Elsevier: London, 1988; p 3.
(4) Flory, P. J. *Discuss. Faraday Soc.* **1974**, *57*, 1.
(5) Möller, M.; Mühleisen, E.; Omeis, J. In *Physical Networks and Polymer Gels*; Burchard, W., Ross-Murphy, S. B., Eds.; Elsevier: London, 1990; p 45.
(6) Pedley, A. M.; Higgins, J. S.; Pfeifer, D. G. In *Physical Networks and Polymer Gels*; Burchard, W., Ross-Murphy, S. B., Eds.; Elsevier: London, 1990; p 65.
(7) Wilson, A. D., Prosser, H. J., Eds. *Developments in Ionic Polymers*; Applied Science Publishers: London and New York, 1983.
(8) Mortimer, D. A. *Polym. Int.* **1991**, *25*, 29.
(9) Stadler, R. *Prog. Colloid Polym. Sci.* **1987**, *75*, 140.
(10) Stadler, R.; de Lucca Freitas, L. L. *Colloid Polym. Sci.* **1986**, *264*, 773.
(11) Stadler, R.; de Lucca Freitas, L. L. *Polym. Bull.* **1986**, *15*, 173.
(12) de Lucca Freitas, L. L.; Burgert, J.; Stadler, R. *Polym. Bull.* **1987**, *17*, 431.
(13) Stadler, R.; Burgert, J. *Makroml. Chem.* **1986**, *187*, 1681.
(14) de Lucca Freitas, L. L.; Stadler, R. *Colloid Polym. Sci.* **1988**, *266*, 1095.
(15) Stadler, R.; de Lucca Freitas, L. L. *Colloid Polym. Sci.* **1988**, *266*, 1102.
(16) Stadler, R.; de Lucca Freitas, L. L. *Macromolecules* **1987**, *20*, 2478.
(17) Brandrup, J.; Immergut, E. H. *Polymer Handbook*, 3rd ed.; Wiley-Interscience: New York, 1989.
(18) Stickler, J. C.; Pirkle, W. H. *J. Org. Chem.* **1966**, *31*, 3444.
(19) Cookson, R. G., Gupte, S. S. *Org. Synth.* **1971**, *51*, 121.
(20) Zinner, G.; Denker, W. *Arch. Pharm.* **1961**, *294*, 370.
(21) Burgert, J. Ph.D. Thesis, Albert-Ludwigs-Universität, Freiburg, Germany, 1988.
(22) Butler, G. B.; Williams, A. G. *J. Polym. Sci., Polym. Chem. Ed.* **1979**, *17*, 1117.
(23) Butler, G. B.; Leong, K. W. *J. Macromol. Sci., Chem.* **1980**, *A14* (3), 287.
(24) Butler, G. B.; Leong, K. W.; Ohashi, S.; Matyjaszewski, K. *J. Org. Chem.* **1980**, *45*, 3467.
(25) Zimm, B. H. *J. Chem. Phys.* **1948**, *16*, 1093.
(26) Zimm, B. H. *J. Chem. Phys.* **1948**, *16*, 1099.
(27) Burchard, W. *Chimia* **1985**, *39*, 10.
(28) Burchard, W.; Richtering, W. *Prog. Polym. Colloid Sci.* **1989**, *80*, 151.
(29) Burchard, W. *Makromol. Chem., Macromol. Symp.* **1988**, *18*, 1.
(30) Tanford, C. *Physical Chemistry of Macromolecules*; John Wiley & Sons: New York and London, 1961.
(31) Huber, K.; Burchard, W.; Bantle, S.; Lutz, P. *Macromolecules* **1985**, *18*, 1461.
(32) de Gennes, P.-G. *Scaling Concepts in Polymer Physics*; Cornell University Press: Ithaca, NY, 1979.
(33) Burchard, W.; Bantle, S. *Polymer* **1986**, *27*, 733.
(34) Burchard, W.; Schulz, L. *Das Papier* **1989**, *43*, 665.
(35) Burchard, W. *Makromol. Chem., Macromol. Symp.* **1990**, *20*, 179.
(36) Burchard, W.; Lang, P.; Auersch, A.; Littke, W. *J. Cryst. Growth* **1991**, *110*, 201.
(37) Yamakawa, H. *Modern Theory of Polymer Solutions*; Harper & Row: New York, 1971.
(38) Carnahan, N. F.; Starling, V. E. *J. Chem. Phys.* **1969**, *51*, 635.
(39) Friedman, H. L. *A Course in Statistical Mechanics*; Prentice-Hall: Englewood Cliffs, NJ, 1985.
(40) Freed, K. F. *Renormalization Group Theory of Macromolecules*; John Wiley & Sons: New York, 1987.
(41) McQuarrie, D. A. *Statistical Mechanics*; Harper & Row: New York, 1973.
(42) Carpenter, D. K. *Encyclopedia of Polymer Science and Technology*; Wiley: New York, 1970; Vol. 12, p 626.
(43) Burchard, W.; Schulz, L.; Auersch, A.; Littke, W. *Polym. Prepr. (Am. Chem. Soc., Div. Polym. Chem.)* **1990**, *31* (2), 131.
(44) Flory, P. J. *Principles in Polymer Chemistry*; Cornell University Press: Ithaca, NY, and London, 1953.
(45) Stockmayer, W. H. *J. Chem. Phys.* **1943**, *11*, 45.
(46) de Lucca Freitas, L. L. Ph.D. Thesis, Albert-Ludwigs-Universität, Freiburg, Germany, 1989.
(47) Stadler, R.; de Lucca Freitas, L. L.; Abetz, V.; Auschra, C. *Colloid Polym. Sci.* **1991**, *269*, 566.